Journal of Alloys and Compounds 509 (2011) 2518–2522

Contents lists available at ScienceDirect

Journal of Alloys and Compounds

journal homepage: www.elsevier.com/locate/jallcom

A Maxwell-pulse constitutive model of $Zr_{55}Cu_{30}Al_{10}Ni_5$ bulk metallic glasses in supercooled liquid region

Xin-yun Wang*, Na Tang, Zhi-zhen Zheng, Ying-ying Tang, Jian-jun Li, Lin Liu

State Key Laboratory of Material Processing and Die & Mould Technology, Huazhong University of Science and Technology, 1037 Luoyu, Hongshan District, 430074 Wuhan, Hubei, China

ARTICLE INFO

Article history:
Received 9 June 2010
Received in revised form 9 November 2010
Accepted 11 November 2010
Available online 19 November 2010

Keywords:
Bulk metallic glass
Modeling
Stress overshoot
Micro-backward extrusion
Finite element analysis

ABSTRACT

Stress overshoot related to the variation in free volume is an important phenomenon in cylinder compression tests of bulk metallic glasses (BMGs). A Maxwell-pulse constitutive model was proposed according to the overshoot of $Zr_{55}Cu_{30}Al_{10}Ni_5$ BMG in the supercooled liquid region (SCLR). Compression experiments and the constitutive model showed good agreement, especially with regard to the stress overshoot phenomenon. Furthermore, micro-backward extrusion experiments and numerical simulation were conducted in SCLR. The results showed that the constitutive model describes the mechanical behavior of the BMG well.

1. Introduction

The unique mechanical properties of bulk metallic glasses (BMGs) have attracted an increasing amount of attention. Although BMGs possess very low plasticity at room temperature, they show good deformation ability in a certain temperature range [1,2], that is, in the supercooled liquid region (SCLR). So thermoplastic forming is an effective method for widening the applications of BMGs into machinery, telecommunications, aerospace, automobile, chemical, sports equipment and military fields [3–5].

Many papers have studied the effects of temperature and strain rate on their flow behavior and deformation ability during thermoplastic forming, [6–10]. Recent research has found that friction condition, shape design and shock loading can also affect the plastic deformation flow of BMGs [11–13]. A standard method has also been proposed to describe the formability of different BMGs by assessing their maximum diameter in compression testing [14]. Because of their unique formability in SCLR, BMGs have been widely used for experimental processing, including indentation or nanoindentation [15–20], joining [21], rolling [22], torsion [23], extrusion [24], bending [25], and microforming [26–30].

However, many recent experimental studies on thermoplastic forming of BMGs have been conducted through trial and error. As the thermoplastic forming process of BMGs in SCLR is sensitive to the variation of processing parameters, a numerical calculation method is needed to simulate and accurately predict the deformation behavior of BMGs. Therefore, research into a constitutive model which can be used to construct a finite element (FE) simulation model with regard to the thermoplastic forming of BMGs has attracted growing attention [31,32]. Since Spaepen was first to establish the free volume model of glassy materials which corresponds to the thermoplastic deformation mechanism on atomic scale, many scholars have put forward their own constitutive models to forecast the plastic flow behavior of BMGs in SCLR. Kawamura et al. presented a stretched exponential model according to the Arrhenius relation, which can describe the steady-state flow stress well, but cannot express the equilibrium viscosity over the entire temperature range [33]. The model that Lu et al. presented can fit the stress overshoot phenomenon only under a high strain rate [34]. Kim et al. used a fictive stress model to predict the peak stress and steady state stress values and proposed a free volume based constitutive model by a finite element method, which matched well the experimental data for a Pd-based BMG [32,35]. Gun et al. used the Zener–Hollomon parameter, Z, to determine the optimum conditions for superplastic flow in the material [36]. In recent years, Anand et al. put forward a Coulomb–Mohr type constitutive theory, which can be used for the entire temperature range [37–40]. However, the model is often too complex to apply.

Until now, there has not been a very good constitutive model to describe the steady flow and stress overshoot at the same time. In this paper, a Maxwell-pulse constitutive model was put forward, according to the thermoplastic deformation behavior of

* Corresponding author. Tel.: +86 27 87543491; fax: +86 27 87543491.
E-mail address: bigaxun@263.net (X.-y. Wang).

0925-8388/$ – see front matter © 2010 Published by Elsevier B.V.
doi:10.1016/j.jallcom.2010.11.070

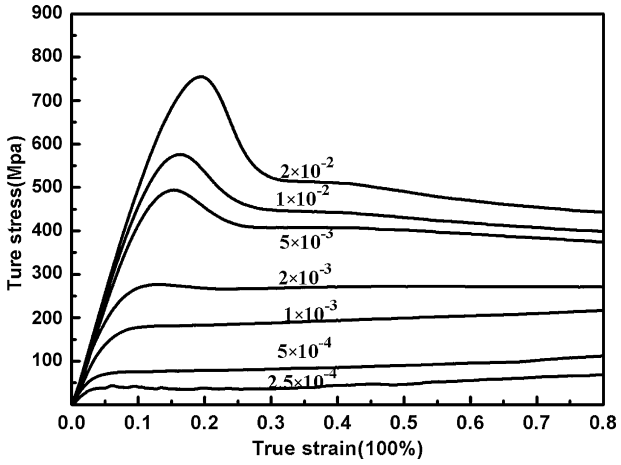

Fig. 1. True stress–strain curves at a temperature of 694 K with different strain rates.

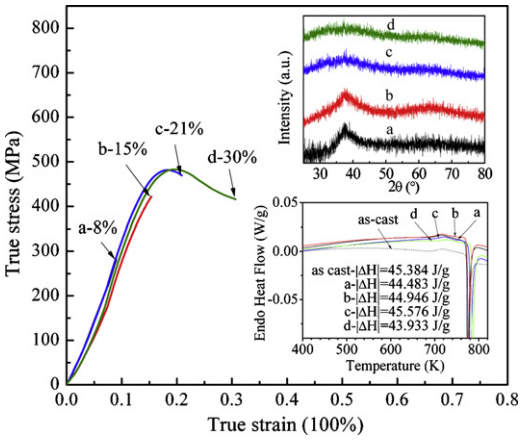

Fig. 2. XRD patterns and DSC traces of deformed samples at strain rate of 0.01 s^{-1} and temperature 694 K.

$Zr_{55}Cu_{30}Al_{10}Ni_5$ BMG in the supercooled liquid region, which combined a visco-elastic Maxwell model and pulse functions. In this model, a fictive stress model was used to construct the relationship between flow stress, strain rate and temperature. Thereafter, the constitutive model was written into the FE software MSC/Marc to predict the deformation force of a micro-backward extrusion process. Subsequently, comparison experiments with the same deformation parameters were conducted in SCLR.

2. Experimental details

A copper casting mold was used to prepare $Zr_{55}Cu_{30}Al_{10}Ni_5$ BMG cylinders with a diameter of 3 mm. X-ray diffraction analysis (XRD, Philips, X'Pert Pro) and differential scanning calorimetry (DSC, Perkin Elmer DSC 7) at constant heating rate of 20 K/min were used to conduct structural and thermal analyses. The obtained glass transition temperature T_g, crystallization temperature T_x, and SCLR temperature range ΔT_x are 684, 770, and 86 K, respectively. The samples were machined to d 2 mm × 3 mm. The compression test device used was a Zwick/Roell Z200 universal testing machine. In order to study the constitutive relation of BMG in the SCLR, the following strain rates were selected: 2.5×10^{-4}, 5×10^{-4}, 1×10^{-3}, 2×10^{-3}, 5×10^{-3}, 1×10^{-2}, and 2×10^{-2} s^{-1}.

The stress–strain curves of $Zr_{55}Cu_{30}Al_{10}Ni_5$ BMG in the SCLR are shown in Fig. 1. It can be seen that there is a stress-overshoot phenomenon (overshoot) in its initial stage of deformation at a temperature close to T_g. After the stress reached a peak, it declined to a relatively stable plateau. At a certain temperature, both the stress peak and the stable flow stress increased with increasing strain rate, and the difference between the peak stress and the stable stress also gradually increased as the strain rate increased. When the strain rate was lower than 1×10^{-3} s^{-1}, there was no overshoot phenomenon, and the BMG was in Newtonian viscous fluid deformation status. However, the BMG was in a non-Newtonian viscous fluid state at a higher strain rate, and showed a non-linear deformation behavior.

3. Results and discussion

3.1. Variation of free volume

Free volume in a BMG can be termed excess volume compared to an ideal disordered configuration of maximum density, and an atom can move freely in its free volume without a change in its energy [41]. After an external stress has acted on a BMG in SCLR, a certain free volume can be created by squeezing an atom with hard-sphere volume into a neighboring site with a smaller volume. At the same time, a relaxation process along with structural rearrangement leads to an annihilation of free volume [42].

So, the change of the overshoot phenomenon at different strain rates in Fig. 1 may be related to the variation of free volume in the BMG. A hypothetical physical phenomenon is posited: before and after stress overshoot, the free volume value will change inside the BMG material. Before the stress reaches its peak, the amount of free volume generated is less than that of annihilation by diffusion, which leads to an increase in stress. As the production of free volume increases rapidly, the amount generated is greater than that of annihilation, so the stress value begins to decrease. Finally, when the amount of free volume generated equals the annihilation amount, the stress value decreases to a steady-state flow stress.

Van den Beukel and Sietsma related the variation of free volume in BMG to the glass transition observed in a DSC measurement [43]. The effect of thermoplastic forming parameters on deformation behavior of BMGs has been discussed based on free volume theory [44,45]. The changes of enthalpy are proportional to the variation of free volume per atom [46–50]. The enthalpy increases with the increasing free volume. Based on the measured enthalpy change of deformed BMG during a constant heating rate DSC test, the variation of free volume can be determined.

Fig. 2 shows the XRD patterns and DSC traces of the samples with selected pre-strains of 8%, 15%, 21% and 30%, which are around the overshoot strain. The pre-stain was conducted by compression at a temperature of 694 K and a strain rate of 1×10^{-4} s^{-1}. From the XRD insert in Fig. 2, it can be seen that all pre-strained samples are in a single amorphous phase state, because no peak corresponding to a crystalline phase can be observed. The lower inset in Fig. 2 shows that enthalpy change increases with the increase in pre-strain value, and reaches the maximum value of 45.576 J/g at a pre-strain of 21%. Thereafter, the enthalpy change decreases to 43.933 J/g at a pre-strain of 30%. This pattern of change for enthalpy, which shows an increase at first and then a decrease, is similar to that of stress in Fig. 2. According to the relation between enthalpy change and free volume variation mentioned above, this pattern indicates that free volume may be subject to a similar variation rule. In other words, the variation of free volume is affected by strain, and the hypothetical physical phenomenon mentioned before is proper. It implies that an equation can be constructed to interrelate free volume and strain. This will be discussed in the next section.

3.2. Constitutive equation

According to the relation between reduced free volume and temperature in equilibrium [43], $x_{eq} = f(T)$, the equilibrium viscosity and flow defect concentration of BMG can be obtained as $\eta_{eq} = \eta_0 \exp(f^{-1}(T))$ and $c_f = \exp(-f^{-1}(T))$, respectively. These three equations can also be interpreted as the relation between flow stress and temperature, because, as is well known, the viscosity of BMG in SCLR is proportional to stress at a particular instant. On the other hand, the strain resulting from an external force affects the variation of free volume [51,52]. Consequently, an equation can be constructed to describe the free volume and strain, $x = f(\varepsilon)$, by

referring to the above three equations. Thereby, a strain related function, $x = (1 - \exp(-(\varepsilon - \varepsilon_0)/t_1))^P \exp(- - (\varepsilon - \varepsilon_0)/t_2))$, can be used to predict the variation of free volume, where ε_0 is the initial strain, t_1 and t_2 are constants related to the strain rate, and P is the attenuation energy used to describe energy dissipation. Then, the stress overshoot phenomenon can be described as a pulse function (see Eq. (1)), which exactly matches the variation of the stress peak.

$$y = y_0 + A\left(1 - \exp\left(-\frac{\varepsilon-\varepsilon_0}{t_1}\right)\right)^P \exp\left(-\frac{\varepsilon-\varepsilon_0}{t_2}\right) \quad (1)$$

where, y_0 is initial stress, A is stress peak amplitude. Because both the height and the width of the stress overshoot peak relate to temperature and strain rate, the characterization of amplitude A consists of strain rate and temperature, which is consistent with the Arrhenius relationship. The abscissa of the peak points can be calculated as,

$$\varepsilon = \varepsilon_0 + t_1 \times (\ln(P \times t_2 + t_1) - \ln(t_1)) \quad (2)$$

Initial strain ε_0 and stress y_0 can be set as zero. The abscissa of the stress overshoot peak is related to the temperature and strain rate. However, the abscissa values of each stress overshoot peak vary little for different temperatures. So, during the fitting process of the parameters, the abscissa values of the stress overshoot peak were set to a constant value of 0.15, according to the condition of strain rate 0.005 s^{-1} and temperature 684 K. So, a pulse function describing the overshoot phenomenon is given as,

$$\sigma_{\text{overshoot}} = K\dot{\varepsilon} \exp\frac{H'}{RT}\left[1 - \exp\left(\frac{-\varepsilon}{t_1}\right)\right]^P \exp\left(\frac{-\varepsilon}{t_2}\right) \quad (3)$$

where K is a structural constant, H' an activation energy.

The Maxwell model is a classic linear visco-elastic constitutive model which consists of a Hooke spring and a Newtonian dashpot. The Hooke spring characterizes the strain ε_E produced by elastic deformation, while the Newtonian dashpot characterizes the strain ε_V produced by plastic deformation. The Maxwell model can describe simple steady-state flow behavior. However, the non-Newtonian flow of BMG in the SCLR is non-linear visco-elastic deformation, and it cannot be expressed exactly by the Maxwell model only. In constructing a constitutive model, the authors used the Maxwell model to characterize the steady-state deformation process:

$$\dot{\sigma} = E\dot{\varepsilon} - \frac{\sigma}{\tau_f} \quad (4)$$

where $\dot{\sigma}$ is stress rate, $\dot{\varepsilon}$ strain rate, E module, and τ_f stress relaxation time. By integrating the Eq. (4), a creep stress equation can be obtained:

$$\sigma_{\text{creep}} = E\tau_f\dot{\varepsilon}\left[1 - \exp\left(\frac{-t}{\tau_f}\right)\right] = \sigma_f\left[1 - \exp\left(\frac{-t}{\tau_f}\right)\right] \quad (5)$$

where σ_f is steady-state flow stress.

$$\sigma_f = 3\dot{\varepsilon}B\exp\left(\frac{H}{RT}\right)\left[1 - \exp\left(\frac{-1}{tA\exp(H*/RT)\dot{\varepsilon}}\right)\right] \quad (6)$$

where B is a constant. Based on the flow behavior of the BMG in the SCLR, a Maxwell-pulse constitutive model is proposed by combining the visco-elastic Maxwell function mentioned above and the pulse function (Eqs. (3) and (5)), as shown in Eq. (7).

$$\sigma(t) = \sigma_{\text{creep}} + \sigma_{\text{overshoot}} \quad (7)$$

Or

$$\sigma = \sigma_f\left[1 - \exp\left(\frac{-\varepsilon}{\tau_f\dot{\varepsilon}}\right)\right] + K\dot{\varepsilon}\exp\frac{H'}{RT}\left[1 - \exp\left(\frac{-\varepsilon}{t_1}\right)\right]^P \exp\left(\frac{-\varepsilon}{t_2}\right) \quad (8)$$

where

$$\tau_f = \frac{\sigma_f}{3E\dot{\varepsilon}} \quad (9)$$

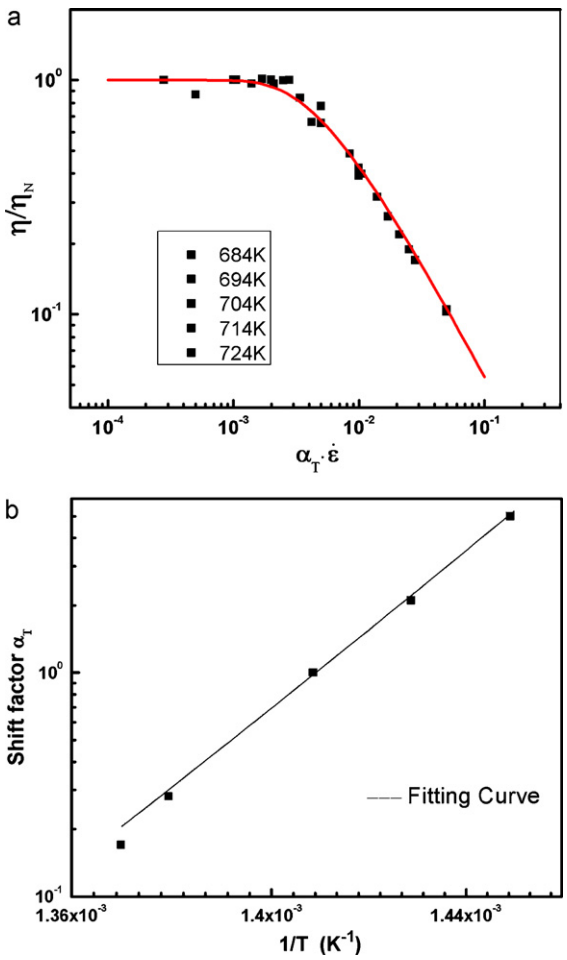

Fig. 3. Processing of parameters fitting: (a) normalization of viscosity and (b) shift factor of fictive stress model.

In this constitutive model, the steady-state flow behavior of the BMG in the SCLR can be fitted very well based on the visco-elastic Maxwell model when considering the effect of stress relaxation during deformation. The strain related pulse function model can characterize the Newtonian viscous fluid deformation state, and the stress overshoot peak in non-Newtonian viscous fluid deformation. So, the Maxwell-pulse model can describe intuitively the flow behavior of the BMG in the SCLR at different temperatures. This model can also be conveniently input into finite element software to analyze the plastic deformation process of the BMG.

3.3. Fitting of parameters

There are several methods for solving steady-state flow stress, for example, the free volume model, the stretched exponential function, and the fictive stress model. Because the flow stress calculated from the fictive stress model is closer to experimental values, the parameters of the flow stress equation can be obtained by fitting the fictive stress model. The construction of the fictive stress model is based on stress relaxation, which can fit Newtonian fluid and non-Newtonian fluid behavior. Kato et al. [53] used a finite element method to validate the applicability of the fictive stress model; the fitting values agreed with experimental results very well.

The fictive stress model normalizes steady-state viscosity η_f at different temperatures by equilibrium viscosity η_N, then a shift factor α_T is used to normalize the curves of different strain ratio $\dot{\varepsilon}$ to the master one (see Fig. 3).

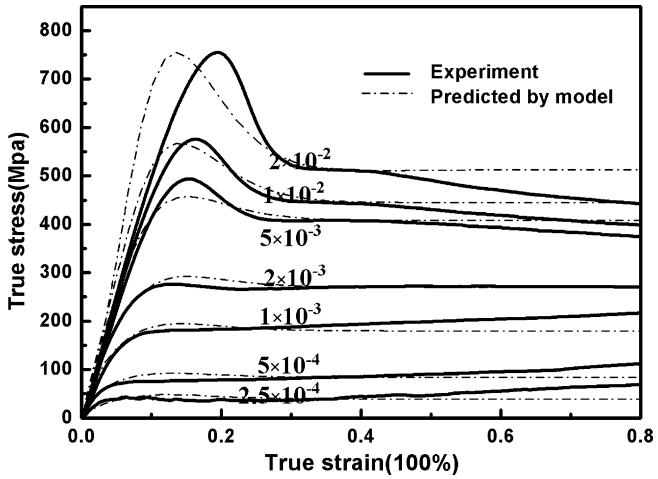

Fig. 4. Comparison of predicted results and experimental data at different strain rates.

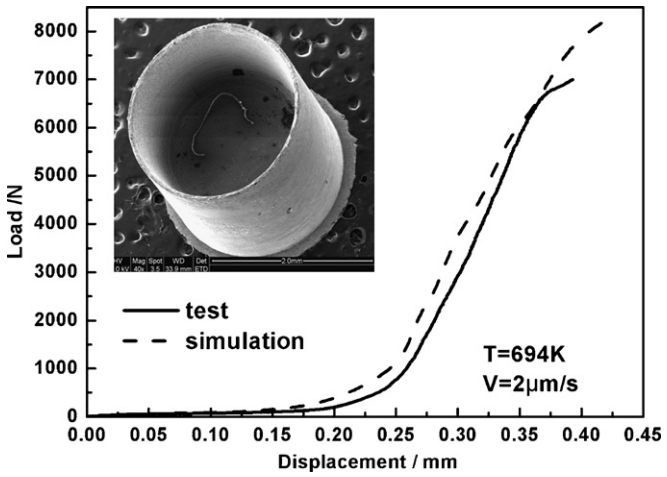

Fig. 6. Experimental and simulated load–displacement curves of micro-backward extrusion cup.

The fitting parameters of the fictive stress model are $B = 6.03 \times 10^{-19}$, $H = 388$ kJ/mol, $A = 1.58 \times 10^{-25}$, $H^* = 337$ kJ/mol and $t = 180$ s, respectively. Other parameters are fitted to be $K = 7.4 \times 10^{-18}$, $t_1 = 5.1$, $t_2 = 0.03$, $P = 4.1$ and $H' = 394$ kJ/mol, respectively, according to the high temperature compression test data.

3.4. Validation with simple cylinder compression test

Based on the proposed Maxwell-pulse constitutive model, the authors fitted the true stress–strain curve of different strain rates of the BMG in the SCLR. The stress–strain curves at different strain rates are shown in Fig. 4. Dashed lines show those calculated from the constitutive model, while solid lines show curves obtained from the compression experiment. From Fig. 4, it can be seen that the curves of the proposed Maxwell-pulse constitutive model show a very good agreement with that of the experiment of the BMG in the SCLR, including the Newtonian flow behavior and the transition from non-Newtonian to Newtonian flow, which plays a key role in the application of $Zr_{55}Cu_{30}Al_{10}Ni_5$ BMG in high temperature forming.

The finite element simulation software MSC/Marc was selected to simulate the compression tests of $Zr_{55}Cu_{30}Al_{10}Ni_5$ BMG in the SCLR, the proposed Maxwell-pulse constitutive model can be input directly into the FE software. The applicability of the constitutive

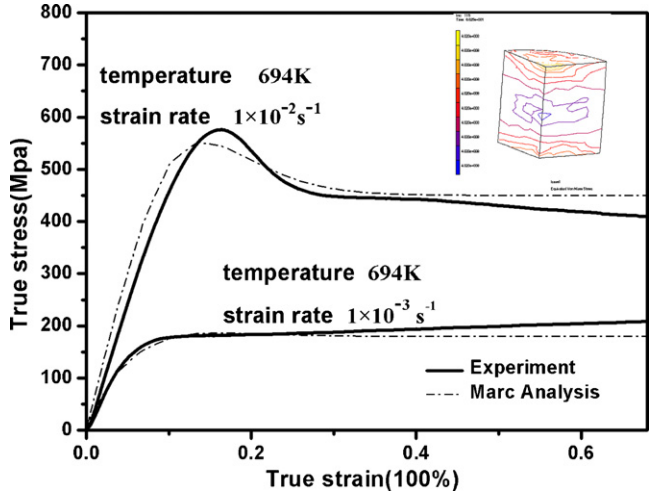

Fig. 5. Comparison of simulated results and experimental data.

model was verified by comparing the experimental data and the FE-calculated results. Because of the symmetry of the compression test specimen, only 1/4 of the solid model was used in the simulation. The three-dimensional solid was meshed with a tetrahedral mesh. Simulation parameters were set according to the compression test conditions in Fig. 1, and the friction coefficient was set to be 0.5.

Fig. 5 shows a comparison of the simulation curves and the true stress–strain curves under the conditions of the strain rate of 0.001 s^{-1} and 0.01 s^{-1} at a temperature of 694 K. Contrasting the Marc numerical simulation results and the experimental values, it can also be seen that Maxwell-pulse constitutive model provides a good fit for the Newtonian and non-Newtonian flow behavior of the BMG in the SCLR.

3.5. Validation with micro-backward extrusion test

Through the above research and analysis, it was shown that the proposed Maxwell-pulse constitutive model can be used to describe the simple cylinder compression forming of the BMG in the SCLR. This section will introduce a more complex deformation process of a backward extruded cup with a very thin wall to evaluate the proposed model by experiment and FE simulation.

Samples were machined to a diameter of 2.18 mm and a height of 1.2 mm. Then a backward extrusion experiment was conducted to make a micro-size cup on the Zwick/Roell mechanical testing machine.

Fig. 6 shows the load–displacement curves of the micro-backward extrusion test and FE simulation at a temperature of 694 K and an extrusion rate of 2 μm s^{-1}. The insert is a scanning electron micrograph of an extruded cup with an outside diameter of 2.2 mm and a wall thickness of 50 μm. It can be seen that the extruded sample has a uniform wall thickness and a high surface finish after forming. The load data simulated with the proposed constitutive model agree well with the experimental results. So, the Maxwell-pulse constitutive model constructed in the paper is accurate, and can be used for the study of the $Zr_{55}Cu_{30}Al_{10}Ni_5$ BMG material in plastic deformation.

4. Conclusions

The flow behavior of $Zr_{55}Cu_{30}Al_{10}Ni_5$ BMG in the SCLR can be divided into Newtonian flow and non-Newtonian flow. Under a certain deformation condition, the stress overshoot phenomenon will appear during deformation in the SCLR.

(1) A Maxwell-pulse constitutive model for $Zr_{55}Cu_{30}Al_{10}Ni_5$ BMG in the SCLR was proposed and the parameters in constitutive model were obtained using a fitting method.
(2) The proposed model fitted the deformation behavior not only in the Newtonian flow region but also in the process of changing from Newtonian flow to non-Newtonian flow.
(3) Numerical simulation and the micro-backward extrusion cup experiment proved that the Maxwell-pulse constitutive model proposed in this paper can describe the thermoplastic deformation behavior of the $Zr_{55}Cu_{30}Al_{10}Ni_5$ BMG in the SCLR.

Acknowledgements

This research was supported by the NSFC (50635020), and the Key Project of the Chinese Ministry of Education (107075).

References

[1] Y. Huang, J. Shen, Y. Sun, J. Sun, J.J.J. Chen, J. Alloys Compd. 504S (2010) S82–S85.
[2] M.M. Trexler, N.N. Thadhani, Prog. Mater. Sci. 55 (2010) 759–839.
[3] J. Schroers, Adv. Mater. 22 (2010) 1566–1597.
[4] J. Ragani, A. Volland, S. Valque, Y. Liu, S. Gravier, J.J. Blandin, M. Suéry, J. Alloys Compd. 504S (2010) S267–S270.
[5] X.D. Wang, J.Z. Jiang, H. Franz, J. Alloys Compd. 483 (2009) 132–135.
[6] Y. Kawamura, T. Nakamura, A. Inoue, Scripta Mater. 39 (1998) 301–306.
[7] Y. Kawamura, T. Shibata, A. Inoue, T. Masumoto, Acta Mater. 46 (1998) 253–263.
[8] Q.S. Zhang, W. Zhang, G.Q. Xie, D.V. Louzguine-Luzgina, A. Inoue, Acta Mater. 58 (2010) 904–909.
[9] F. Yuan, V. Prakash, J.J. Lewandowski, Mech. Mater. 42 (2010) 248–255.
[10] P.J. Tao, Y.Z. Yang, X.J. Bai, Z.W. Xie, X.C. Chen, Mater. Lett. 64 (2010) 1421–1423.
[11] S. Scudino, K.B. Surreddi, G. Wang, J. Eckert, Scripta Mater. 62 (2010) 750–753.
[12] N.H. Tariq, J.I. Akhter, B.A. Hasan, M.J. Hyderc, J. Alloys Compd. 507 (2010) 414–418.
[13] S.A. Atroshenko, N.F. Morozov, W. Zheng, Y.J. Huang, Y.V. Sudenkov, N.S. Naumova, J. Shen, J. Alloys Compd. 505 (2010) 501–504.
[14] J. Schroers, Acta Mater. 56 (2008) 471–478.
[15] G. Kumar, H.X. Tang, J. Schroers, Nat. Lett. 457 (2009) 868–872.
[16] K. Chen, J. Lin, Int. J. Plasticity 26 (2010) 1645–1658.
[17] V. Keryvin, X.D. Vu, V.H. Hoang, J. Shen, J. Alloys Compd. 504S (2010) S41–S44.
[18] B. Yoo, K. Lee, J. Jang, J. Alloys Compd. 483 (2009) 136–138.
[19] K.W. Chen, S.R. Jian, P.J. Wei, J.S.C. Jang, J.F. Lina, J. Alloys Compd. 504S (2010) S69–S73.
[20] S. Nowak, P. Ochin, A. Pasko, O. Maciejak, P. Aubert, Y. Champion, J. Alloys Compd. 483 (2009) 139–142.
[21] P. Kuo, S. Wang, P.K. Liaw, G. Fan, H. Tsang, D. Qiao, F. Jiang, Mater. Chem. Phys. 120 (2010) 532–536.
[22] K.C. Hwang, E.S. Park, M.Y. Huh, H.J. Kim, J.C. Bae, Intermetallics 18 (2010) 1912–1915.
[23] Á. Révész, P. Henits, Z. Kovács, J. Alloys Compd. 495 (2010) 338–340.
[24] Y. Kawamura, H. Kato, A. Inoue, T. Masumoto, Appl. Phys. Lett. 67 (1995) 2008–2010.
[25] N.H. Tariq, B.A. Hasan, J.I. Akhter, M.A. Shaikh, J. Alloys Compd. 479 (2009) 242–245.
[26] Y. Saotome, K. Itoh, T. Zhang, A. Inoue, Scripta Mater. 44 (2001) 1541–1545.
[27] Y. Saotome, S. Miwa, T. Zhang, A. Inoue, J. Mater. Process. Technol. 113 (2001) 64–69.
[28] X. Wu, J.J. Li, Z.Z. Zheng, L. Liu, Y. Li, Scripta Mater. 63 (2010) 469–472.
[29] H.G. Jeong, S.J. Yoo, W.J. Kim, J. Alloys Compd. 483 (2009) 283–285.
[30] D. Wang, G. Liao, J. Pan, Z. Tang, P. Peng, L. Liu, T. Shi, J. Alloys Compd. 484 (2009) 118–122.
[31] P. Thamburaja, R. Ekamabaram, J. Mech. Phys. Solids 55 (2007) 1236–1273.
[32] H.J. Jun, K.S. Lee, S.C. Yoon, H.S. Kim, Y.W. Chang, Acta Mater. 58 (2010) 4267–4280.
[33] Y. Kawamura, T. Nakamura, H. Kato, H. Mano, A. Inoue, Mater. Sci. Eng. A304–A306 (2001) 674–678.
[34] J. Lu, G. Ravichandran, W.L. Johnson, Acta Mater. 51 (2003) 3429–3443.
[35] H.S. Kim, H. Kato, A. Inoue, H.S. Chen, Acta Mater. 52 (2004) 3813–3823.
[36] B. Gun, K.J. Laws, M. Ferry, J. Non-Cryst. Solids 352 (2006) 3896–3902.
[37] L. Anand, C. Su, J. Mech. Phys. Solids 53 (2005) 1362–1396.
[38] C. Su, L. Anand, Acta Mater. 54 (2006) 179–189.
[39] L. Anand, C. Su, Acta Mater. 55 (2007) 3735–3747.
[40] D. Henann, L. Anand, Acta Mater. 56 (2008) 3290–3305.
[41] M.H. Cohen, D. Turnbull, J. Chem. Phys. 31 (1959) 1164–1169.
[42] C.A. Schuh, T.C. Hufnagel, U. Ramamurty, Acta Mater. 55 (2007) 4067–4109.
[43] A. van den Beukel, J. Sietsma, Acta Metall. 38 (1990) 383–389.
[44] B.S.S. Daniel, A. Reger-Leonhard, M. Heilmaier, J. Ecker, L. Schultz, Mech. Time-Depend. Mater. 6 (2002) 193–206.
[45] M. Bletry, P. Guyot, J.J. Blandin, J.L. Soubeyroux, Acta Mater. 54 (2006) 1257–1263.
[46] P. Murali, U. Ramamurty, Acta Mater. 53 (2005) 1467–1478.
[47] A. Slipenyuk, J. Eckert, Scripta Mater. 50 (2004) 46–57.
[48] M.E. Launey, J.J. Kruzic, C. Li, R. Busch, Appl. Phys. Lett. 91 (2007) 0519131–519133.
[49] Q. Chen, L. Liu, K.C. Chan, J. Alloys Compd. 267 (2009) 208–212.
[50] Y. Xu, J. Fang, H. Gleiter, H. Hahn, J. Li, Scripta Mater. 62 (2010) 674–677.
[51] G. Ruitenberg, P. de Hey, F. Sommer, J. Sietsma, Mater. Sci. Eng. A226–A228 (1997) 397–400.
[52] P. de Hey, J. Sietsma, A. van den Beukel, Mater. Sci. Eng. A226–A228 (1997) 336–340.
[53] A. Kato, H. Horikiri, A. Inoue, T. Masumoto, Mater. Sci. Eng. A179–A180 (1994) 707–711.